Electronic Supplementary Information

Experimental section

Materials: tannic acid (TA), palladium dichloride ($PdCl_2$), Hydrochloric acid (HCl), ammonium chloride (NH_4Cl), sodium sulfate (Na_2SO_4), hydrazine hydrate ($N_2H_4 \cdot H_2O$), sodium hypochlorite (NaClO), sodium hydroxide (NaOH), sodium salicylate ($C_7H_5O_3Na$), ethanol (CH_3CH_2OH), and carbon paper were bought from Beijing Chemical Corporation. Para-(dimethylamino) benzaldehyde ($C_9H_{11}NO$), sodium nitroferricyanide (III) dihydrate ($Na_2Fe(CN)_5NO \cdot 2H_2O$) and Nafion were purchased from Aladdin Ltd. (Shanghai, China). The water used throughout all experiments was purified through a Millipore system.

Preparation of Pd and Pd-TA: $H_2PdCl_4 \cdot nH_2O$ was prepared by treating $PdCl_2$ with concentrated hydrochloric acid at 35 °C, in which the molar ratio of $HCl/PdCl_2$ was 2/1. To prepare Pd-TA, 20 mL of tannic acid (1.4×10^{-4} M), 200 uL of H_2PdCl_4 solution were added into a 50 mL beaker and stir at room temperature for 5 minutes. Then add 1 mL fresh 1.2×10^{-4} M of $NaBH_4$ aqueous solution to the above solution. The solution immediately turned dark brown and was stirred at room temperature for 5 min. For comparison, in addition to not adding TA, pure Pd was prepared by the same method.

Preparation of Pd/CP and Pd-TA/CP: CP was cleaned via brief sonication with ethanol and water for several times. 10 mg sample and 40 μL 5 wt% Nafion solution were dispersed in 960 μL water/ethanol (V : V = 1 : 3) followed by 1-h sonication to form a homogeneous ink. 20 μL ink was loaded onto a CP (1×1 cm^2) and dried under ambient condition.

Characterizations: XRD patterns were obtained from a Shimazu XRD-6100 diffractometer with Cu Kα radiation (40 kV, 30 mA) of wavelength 0.154 nm (Japan). TEM images were obtained from a Zeiss Libra 200FE transmission electron microscope operated at 200 kV. XPS measurements were performed on an ESCALABMK II X-ray photoelectron spectrometer using Mg as the exciting source. The absorbance data of spectrophotometer were measured on SHIMADZU UV-1800 ultraviolet-visible (UV-Vis) spectrophotometer.

Electrochemical measurements: Electrochemical measurements were performed with a CHI 660E electrochemical analyzer (CH Instruments, Inc., Shanghai) using a standard three-electrode system using Pd-TA/CP as the working electrode, graphite rod as the counter electrode, and saturated Ag/AgCl electrode as the reference electrode. In all measurements, saturated Ag/AgCl electrode was calibrated with respect to reversible hydrogen electrode as following: in 0.1 M Na_2SO_4 aqueous solution, $E(RHE) = E(Ag/AgCl) + 0.059 \times pH + 0.197$ V. All experiments were carried out at room temperature. For N_2 reduction experiments, the 0.1 M Na_2SO_4 electrolyte was purged with N_2 for 30 min before the measurement. Potentiostatic test was conducted in N_2-saturated 0.1 M Na_2SO_4 solution in a two-compartment cell, which was separated by Nafion 117 membrane.

Determination of NH_3: The produced NH_3 was detected with indophenol blue by ultraviolet spectroscopy[1]. For the ultraviolet spectroscopy, 4 mL electrolyte was obatined from the cathodic chamber and mixed with 50 µL oxidizing solution containing NaClO ($\rho Cl = 4 \sim 4.9$) and NaOH (0.75 M), 500 µL coloring solution containing 0.4 M $C_7H_6O_3Na$ and 0.32 M NaOH, and 50 µL catalyst solution (1 wt% $Na_2[Fe(CN)_5NO]$) for 1 h. Absorbance measurements were performed at $\lambda = 655$ nm. The concentration-absorbance curve was calibrated using standard NH_4^+ solution with a serious of concentrations. The fitting curve ($y = 0.396x + 0.02$, $R^2 = 0.999$) shows good linear relation of absorbance value with NH_4^+ concentration.

Determination of N_2H_4: The N_2H_4 present in the electrolyte was determined by the method of Watt and Chrisp.[2] The mixture of $C_9H_{11}NO$ (5.99 g), HCl (30 mL), and C_2H_5OH (300 mL) was used as a color reagent. In detail, 5 mL electrolyte was removed from the electrochemical reaction vessel, and added into 5 mL above prepared color reagent and stirring 10 min at room temperature. Moreover, the absorbance of the resulting solution was measured at a wavelength of 460 nm. The concentration absorbance curves were calibrated using standard N_2H_4 solution with a series of concentrations. The fitting curve ($y = 0.522x + 0.064$, $R^2 = 0.999$) shows good linear relation of absorbance value with N_2H_4 concentration.

Calculations of NH_3 yield and FE: NH_3 yield was calculated using the following equation:

$$NH_3 \text{ yield} = [NH_3] \times V/(m_{cat.} \times t)$$

FE was calculated according to following equation:

$$FE = 3 \times F \times [NH_3] \times V/(17 \times Q)$$

Where $[NH_3]$ is the measured NH_3 concentration; V is the volume of the cathodic reaction electrolyte; t is the potential applied time; $m_{cat.}$ is the loaded quality of catalyst; F is the Faraday constant; and Q is the quantity of charge in Coulombs.

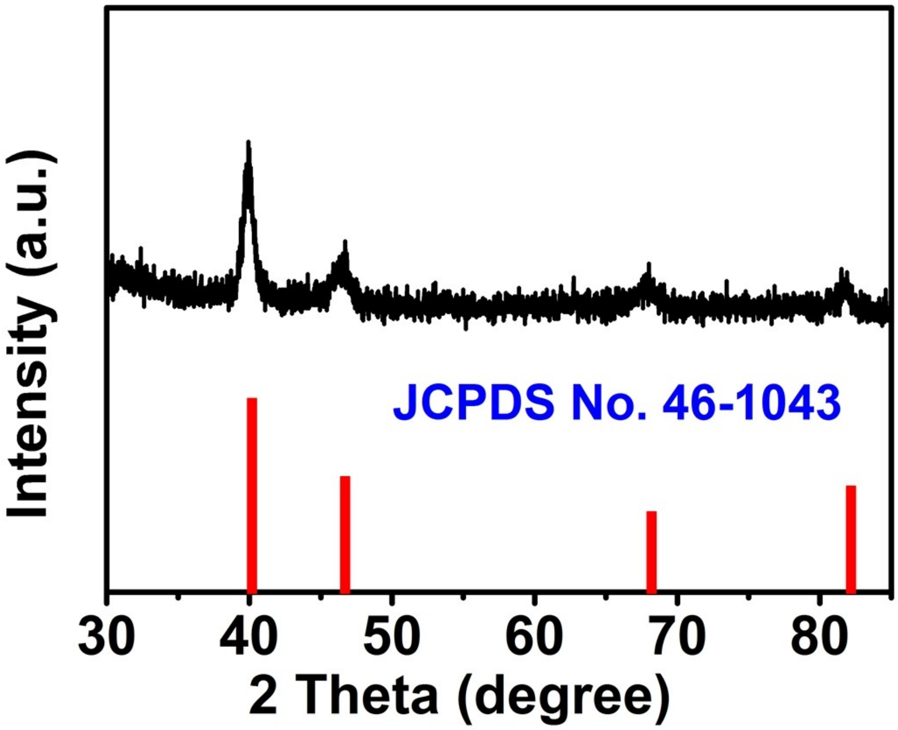

Fig. S1. XRD pattern of pure Pd nanoparticles.

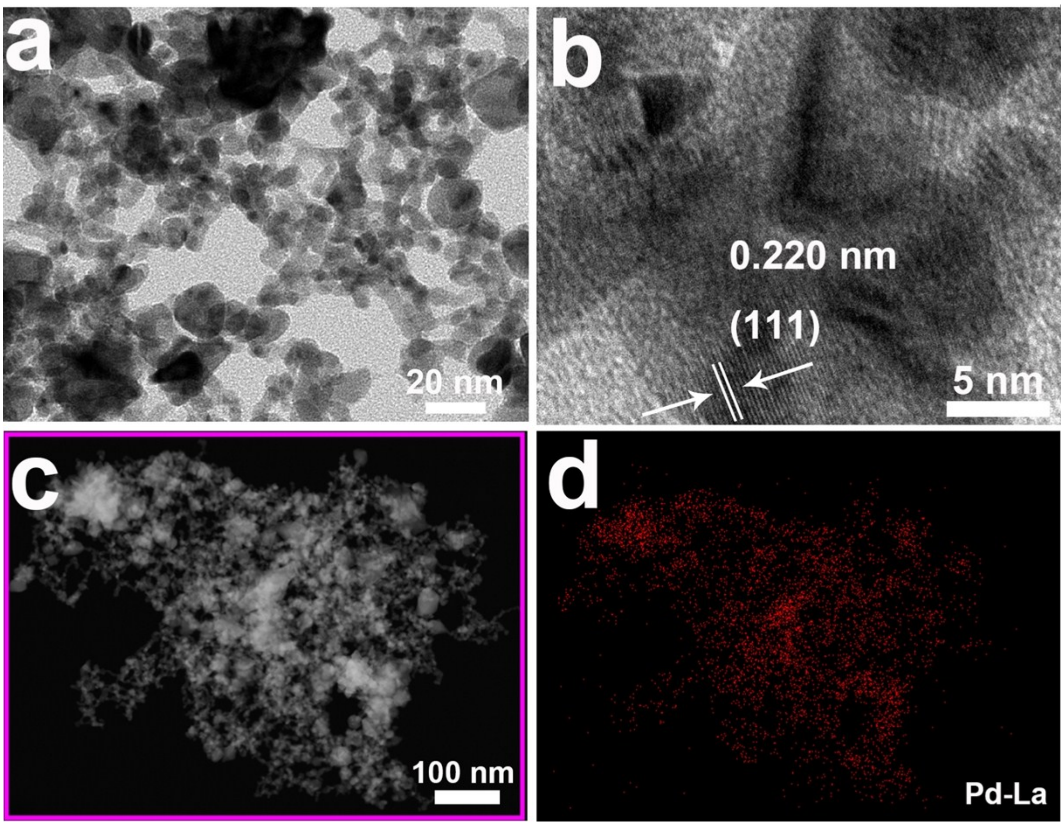

Fig. S2. (a) TEM and (b) HRTEM images for pure Pd nanoparticles. (c) Scanning TEM (STEM) image and (d) corresponding EDX elemental mapping image of Pd for pure Pd nanoparticles.

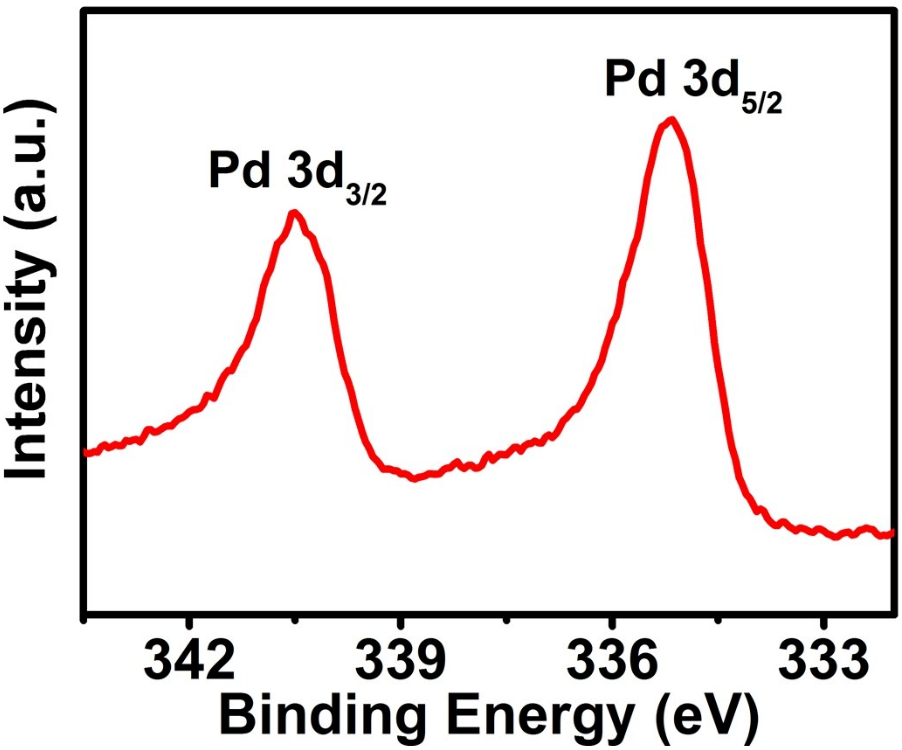

Fig. S3. XPS spectrum of pure Pd in the Pd 3d regions.

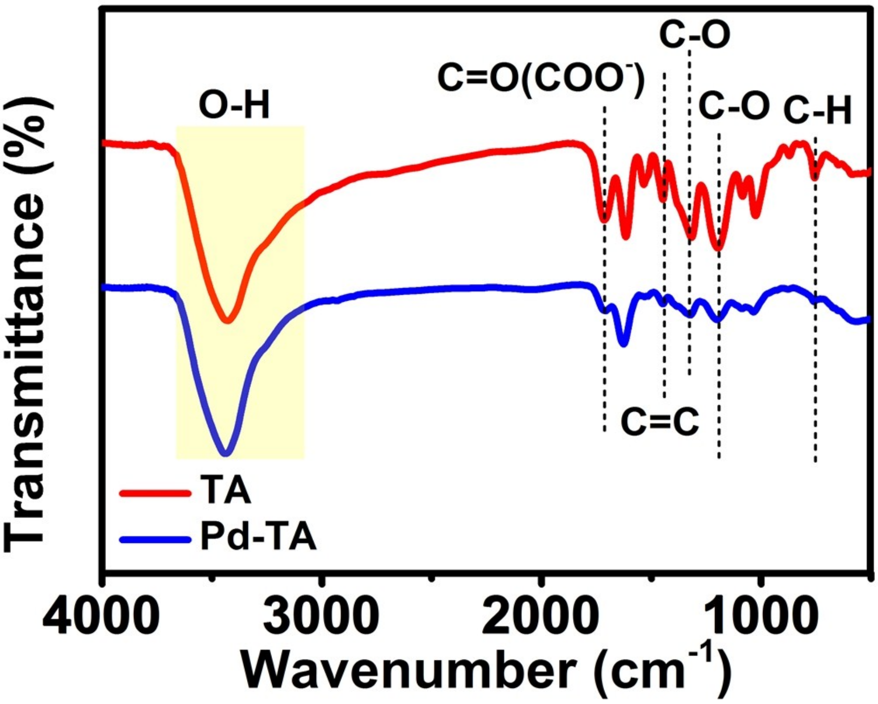

Fig. S4. FT-IR spectra of TA and Pd-TA.

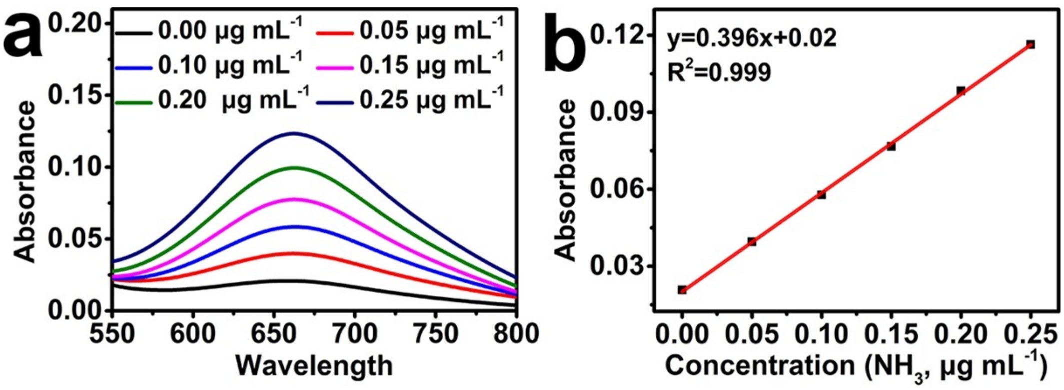

Fig. S5. (a) UV-Vis absorption spectra of indophenol assays with NH_3 concentrations after incubated for 2 h at room temperature. (b) Calibration curve used for calculation of NH_3 concentrations.

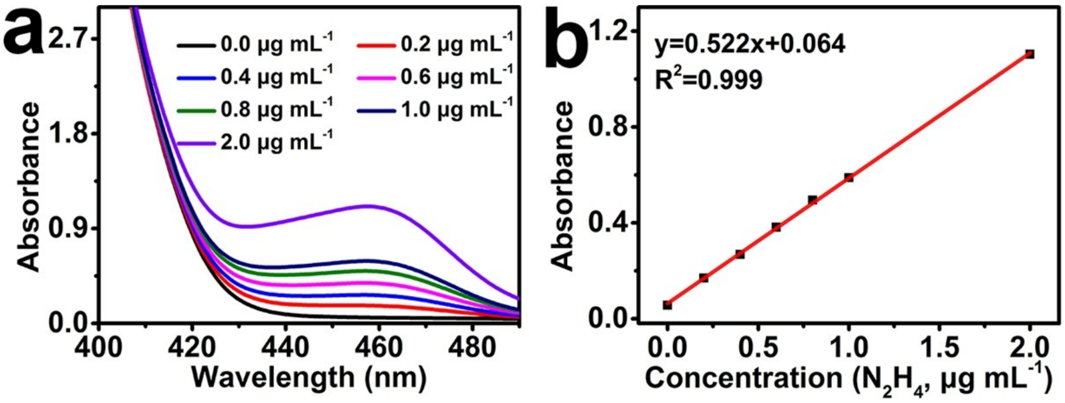

Fig. S6. (a) UV-Vis absorption spectra of various N_2H_4 concentrations after incubated for 10 min at room temperature. (b) Calibration curve used for calculation of N_2H_4 concentrations.

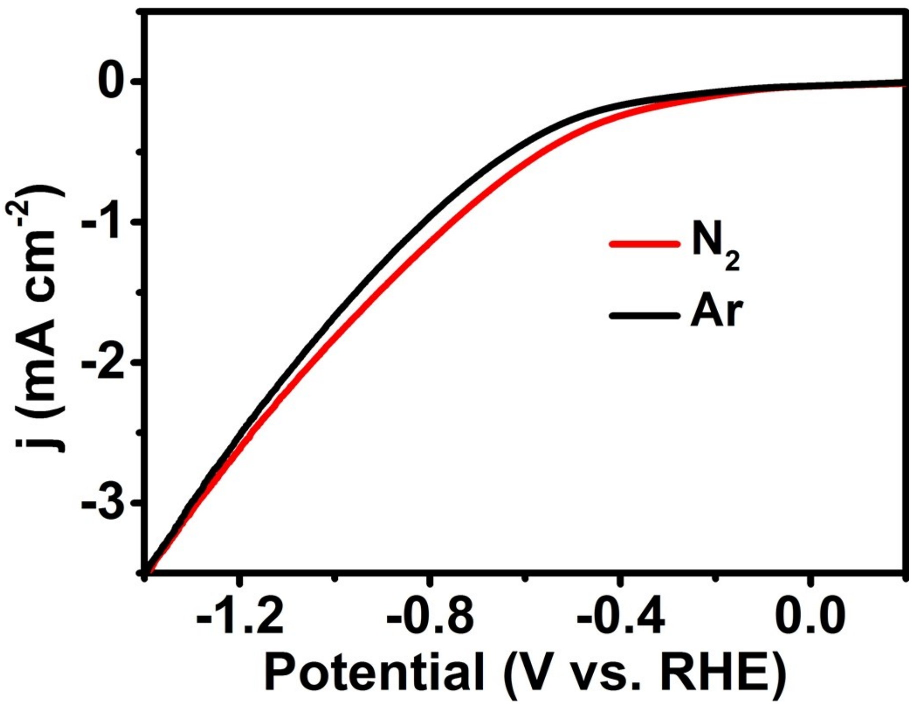

Fig. S7. LSV curves for Pd-TA/CP in Ar- and N_2-saturated 0.1 M Na_2SO_4 with a scan rate of 5 mV s^{-1}.

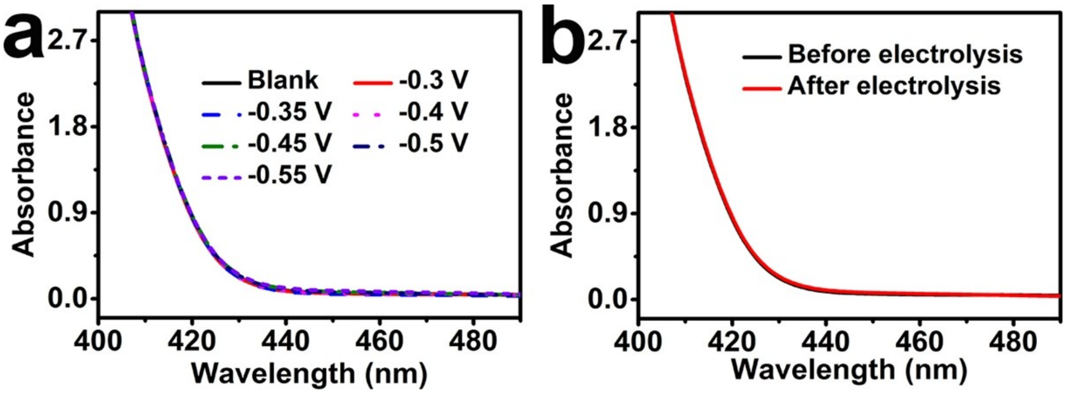

Fig. S8. UV-Vis absorption spectra of the electrolytes stained with p-$C_9H_{11}NO$ indicator after NRR electrolysis at a series of potentials. (a) After 2 h electrolysis at all potentials. (b) After 24 h electrolysis at −0.45 V.

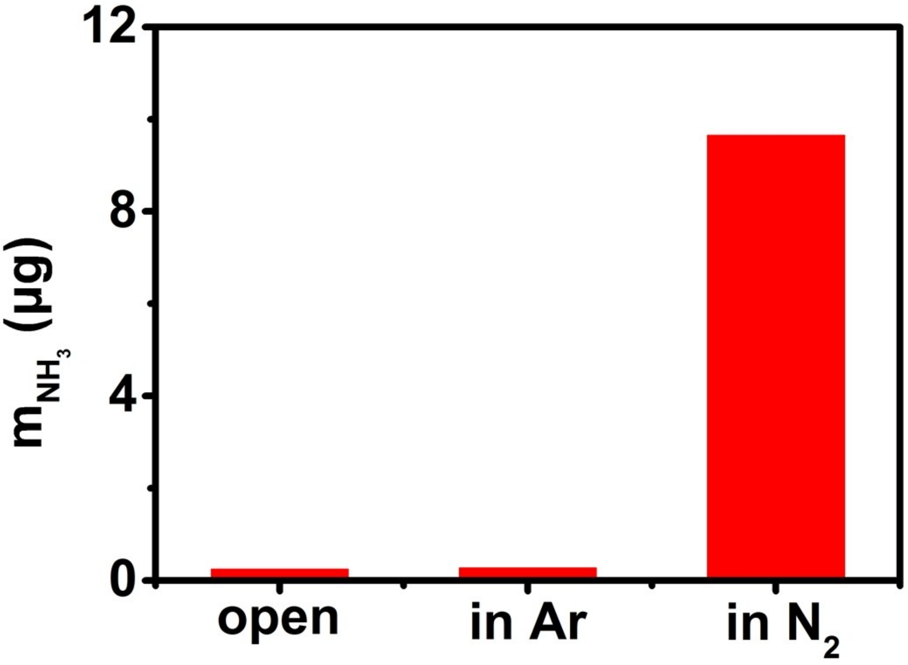

Fig. S9. Amount of NH_3 generated for Pd-TA/CP under different conditions.

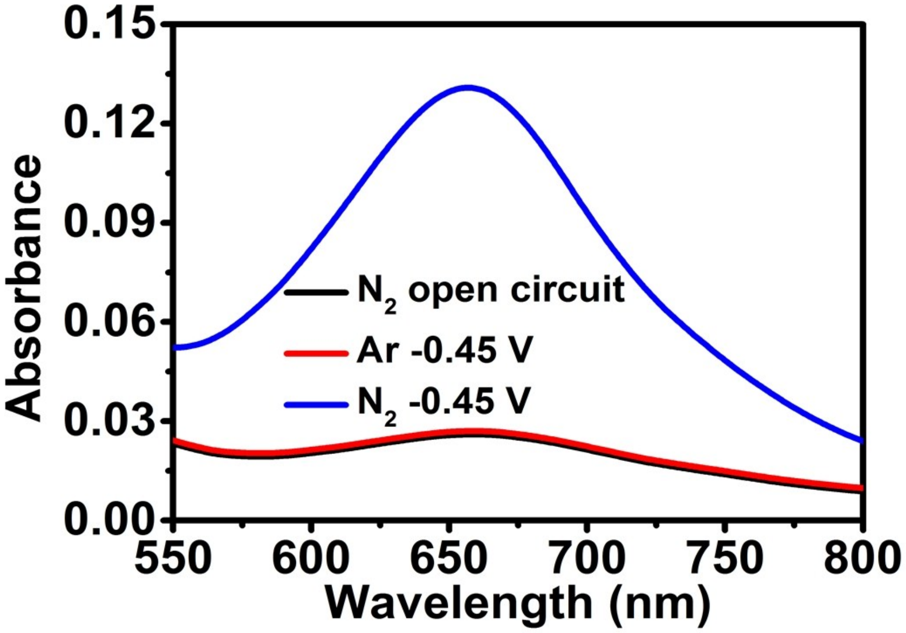

Fig. S10. UV-Vis absorption spectra of 0.1 M Na_2SO_4 electrolyte stained with indophenol indicator after charging at –0.45 V for 2 h under different conditions.

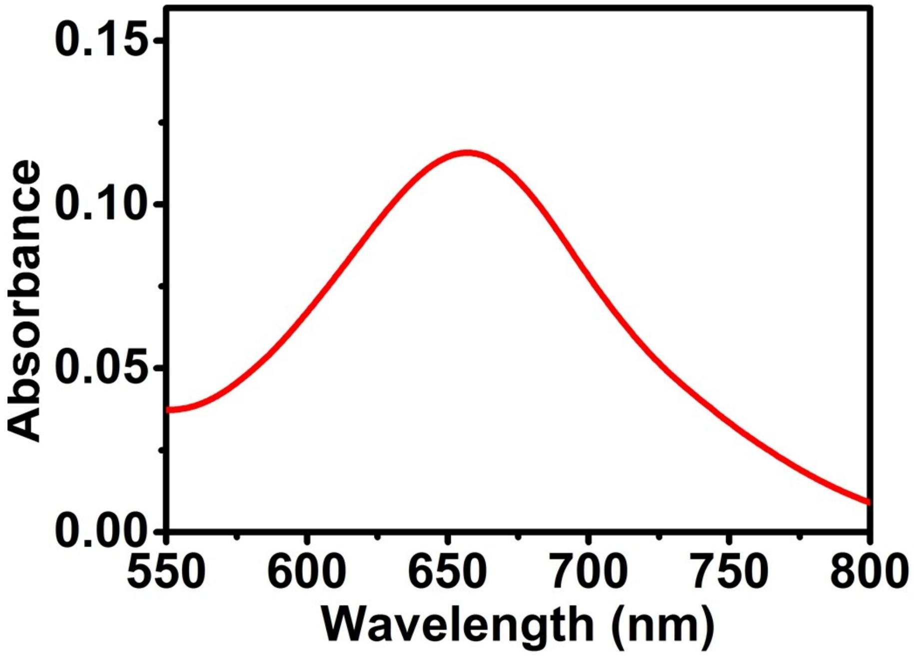

Fig. S11. UV-Vis absorption spectra of electrolyte stained with indophenol indicator after 2 h potentiostatic test at –0.45 V using post-NRR Pd-TA/CP.

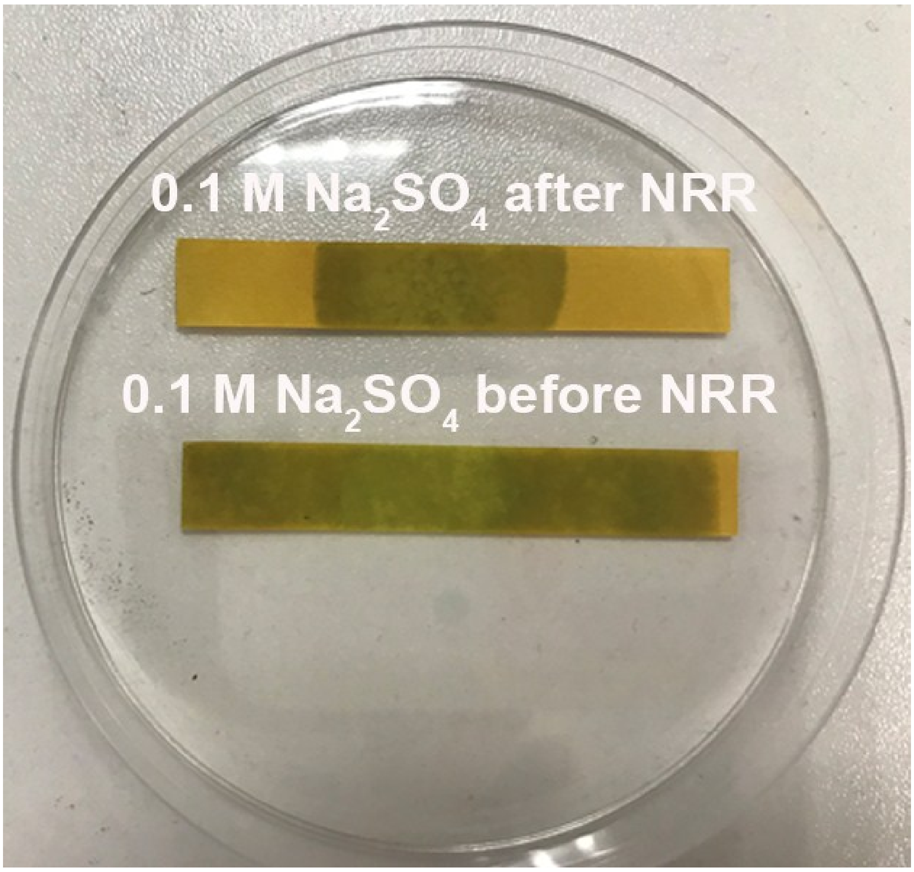

Fig. S12. Photographs of pH test papers in 0.1 M Na_2SO_4 before and after 2 h electrolysis.

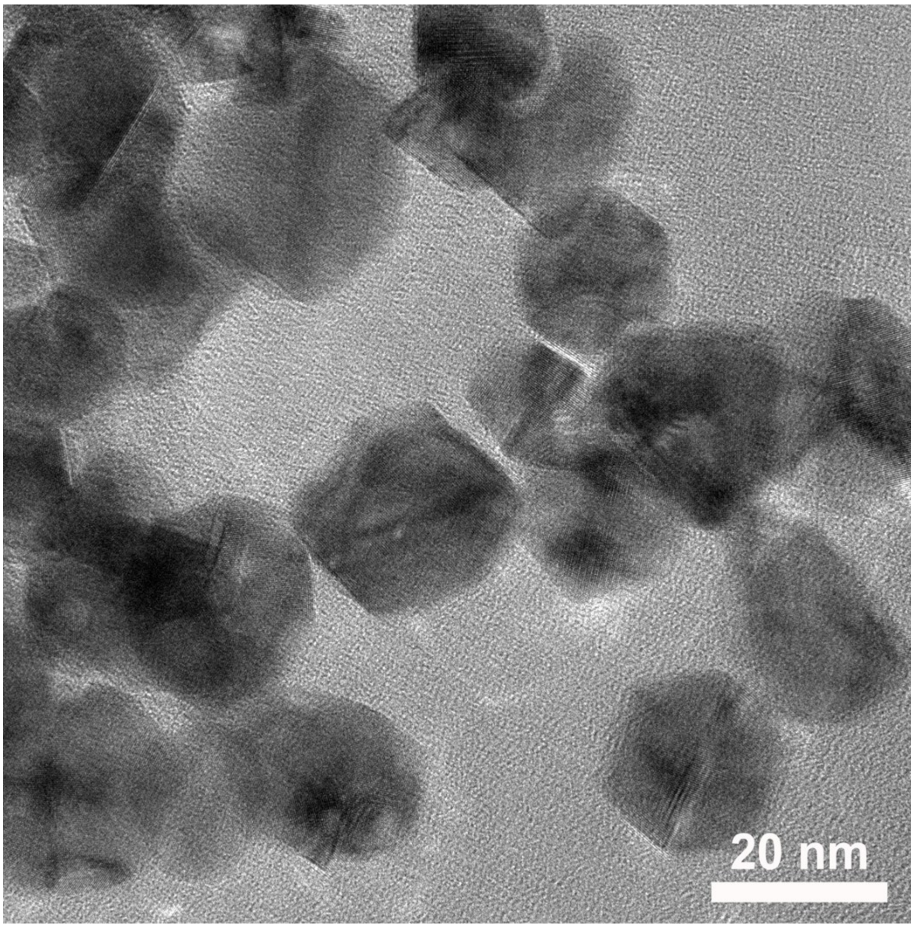

Fig. S13. TEM image for Pd-TA after stability test.

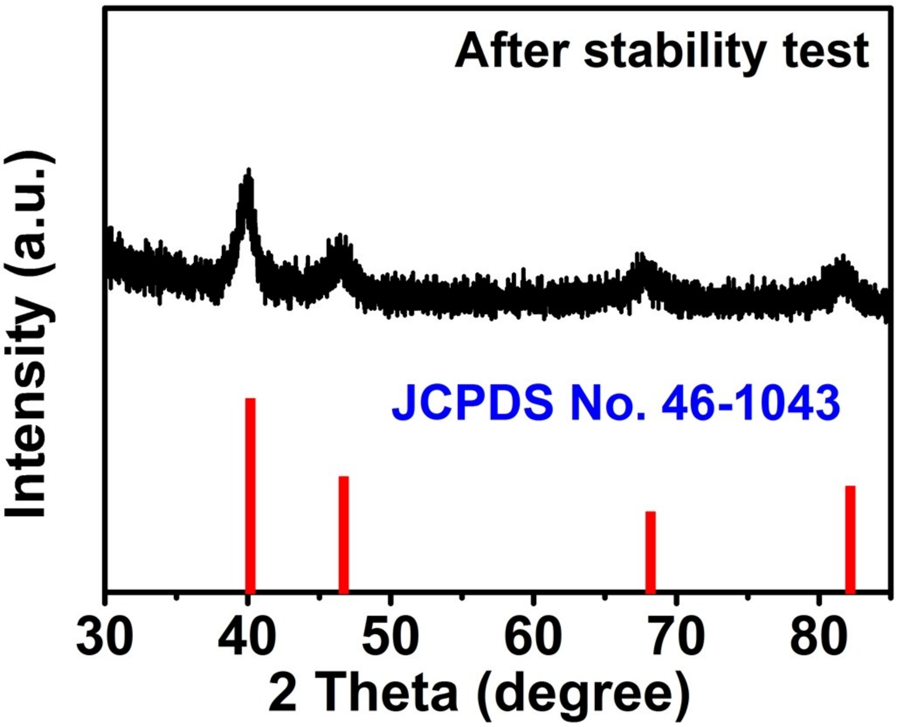

Fig. S14. XRD pattern for Pd-TA after stability test.

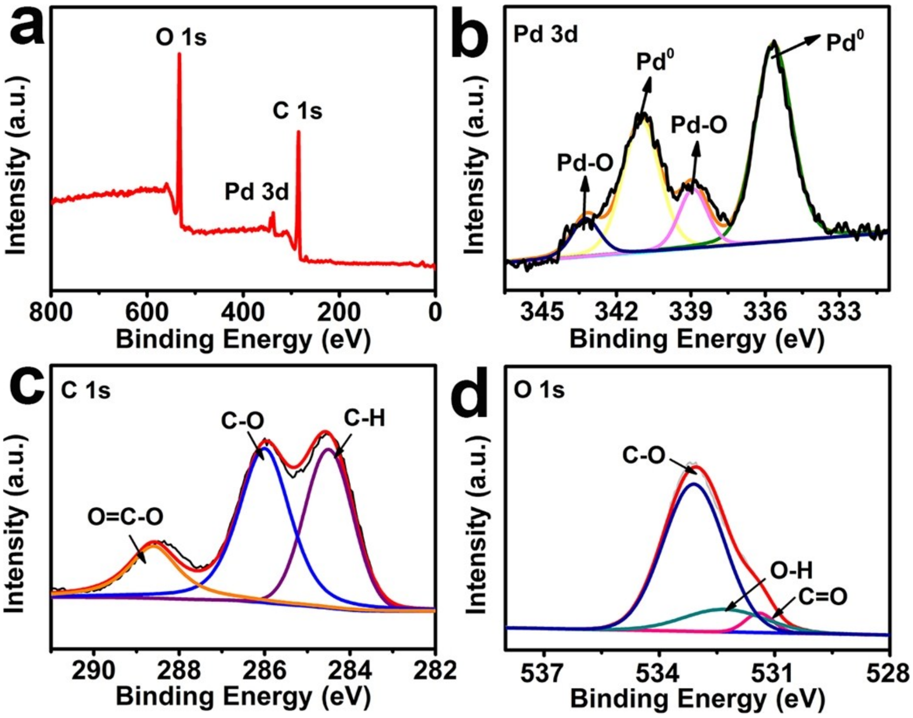

Fig. S15. (a) XPS survey spectrum of Pd-TA after NRR test. XPS spectra of Pd-TA in the (b) Pd 3d (c) C 1s (d) O 1s regions.

Table S1. Comparison of the electrocatalytic NRR performance of Pd-TA with other NRR electrocatalysts under ambient reaction conditions in aqueous media.

Catalyst	Electrolyte	Potential (V) vs. RHE	NH_3 yield	FE(%)	Ref.
Pd-TA	0.1 M Na_2SO_4	−0.45 V	24.12 $\mu g\ h^{-1}\ mg^{-1}_{cat.}$	9.49	This work
Pd/C	0.1 M PBS		4.5 $\mu g\ h^{-1}\ mg^{-1}_{cat.}$ (−0.05 V)	8.2 (0.1 V)	3
$Pd_{0.2}Cu_{0.8}$/rGO	0.1 M KOH		2.8 $\mu g\ h^{-1}\ mg^{-1}_{cat.}$ (−0.2 V)	- (0 V)	4
oxygen-doped carbon nanosheet	0.1 M HCl	−0.6 V	20.15 $\mu g\ h^{-1}\ mg^{-1}_{cat.}$	4.97	5
α-Au/CeO_x-rGO	0.1 M HCl	−0.2 V	8.3 $\mu g\ h^{-1}\ mg^{-1}_{cat.}$	10.1	6
MoO_3	0.1 M HCl		29.43 $\mu g\ h^{-1}\ mg^{-1}_{cat.}$ (−0.5 V)	1.9 (−0.3 V)	7
Au nanorods	0.1 M KOH	−0.2 V	6.04 $\mu g\ h^{-1}\ mg^{-1}_{cat}$	4.02	8
γ-Fe_2O_3	0.1 M KOH	0 V	0.21 $\mu g\ h^{-1}\ mg^{-1}_{cat.}$	1.9	9
Mn_3O_4 nanocube	0.1 M Na_2SO_4	−0.8 V	11.6 $\mu g\ h^{-1}\ mg^{-1}_{cat.}$	3.0	10
MnO	0.1 M Na_2SO_4	−0.39 V	7.92 $\mu g\ h^{-1}\ mg^{-1}_{cat.}$	8.02	11
Nb_2O_5 nanofiber	0.1 M HCl	−0.55 V	43.6 $\mu g\ h^{-1}\ mg^{-1}_{cat.}$	9.26	12
VO_2 hollow microsphere	0.1 M Na_2SO_4	−0.7 V	14.85 $\mu g\ h^{-1}\ mg^{-1}_{cat.}$	3.97	13
Oxygen-doped carbon nanosheet	0.1 M HCl	−0.6 V	20.15 $\mu g\ h^{-1}\ mg^{-1}_{cat.}$	4.97	14
C-TiO_2	0.1 M Na_2SO_4	−0.7 V	16.22 $\mu g\ h^{-1}\ mg^{-1}_{cat.}$	1.84	15
B-TiO_2	0.1 M Na_2SO_4	−0.8 V	14.4 $\mu g\ h^{-1}\ mg^{-1}_{cat.}$	3.4	16
black P nanosheet	0.01 M HCl		31.37 $\mu g\ h^{-1}\ mg^{-1}_{cat.}$	5.07	17

			(−0.7 V)	(−0.6 V)	
Ag nanosheets	0.1 M HCl	−0.6 V	2.83 μg h^{-1} mg$^{-1}_{cat.}$	4.8	18
β-FeOOH nanorod	0.5 M $LiClO_4$		23.32 μg h^{-1} mg$^{-1}_{cat.}$ (−0.75 V)	6.7 (−0.7 V)	19
Fe_3S_4 nanosheets	0.1 M HCl	−0.4 V	75.4 μg h^{-1} mg$^{-1}_{cat.}$	6.45	20
polymeric carbon nitride	0.1 M HCl	−0.2 V	8.09 μg h^{-1} mg$^{-1}_{cat.}$	11.59	21
Au/TiO_2	0.1 M HCl	−0.2 V	21.4 μg h^{-1} mg$^{-1}_{cat.}$	8.11	22
Au flowers	0.1 M HCl	−0.2 V	25.7 μg h^{-1} mg$^{-1}_{cat.}$	6.05	23
$Ti_3C_2T_x$ (T = F, OH)	0.1 M HCl	−0.4 V	20.4 μg h^{-1} mg$^{-1}_{cat.}$	9.3	24
CoP hollow nanocage	1.0 M KOH		10.78 μg h^{-1} mg$^{-1}_{cat.}$ (−0.4 V)	7.36 (0 V)	25
cubic sub–micron SnO_2	0.1 M Na_2SO_4		4.03 μg h^{-1} mg$^{-1}_{cat.}$ (−0.8 V)	2.17 (−0.7 V)	26
hexagonal BN nanosheet	0.1 M HCl	−0.75 V	22.4 μg h^{-1} mg$^{-1}_{cat}$	4.7	27
boron nanosheet	0.1 M Na_2SO_4	−0.8 V	13.22 μg h^{-1} mg$^{-1}_{cat}$	4.04	28
Mn_3O_4 nanoparticles@reduced graphene oxide	0.1 M Na_2SO_4	−0.85 V	17.4 μg h^{-1} mg$^{-1}_{cat}$	3.52	29
S-doped carbon nanosphere	0.1 M Na_2SO_4	−0.7 V	19.07 μg h^{-1} mg$^{-1}_{cat}$	7.47	30

References

1 D. Zhu, L. Zhang, R. E. Ruther and R. J. Hamers, *Nat. Mater.*, 2013, **12**, 836–841.

2 G. W. Watt and J. D. Chrisp, *Anal. Chem.*, 1952, **24**, 2006–2008.

3 J. Wang, L. Yu, L. Hu, G. Chen, H. Xin and X. Feng, *Nat. Commun.*, 2018, **9**, 1795.

4 M. Shi, D. Bao, S. Li, B. Wulan, J. Yan and Q. Jiang, *Adv. Energy Mater.*, 2018, **8**, 1800124.

5 H. Huang, L. Xia, R. Cao, Z. Niu, H. Chen, Q. Liu, T. Li, X. Shi, A. M. Asiri and X. Sun, *Chem. Eur. J.*, 2019, **25**, 1914–1917.

6 S. Li, D. Bao, M. Shi, B. Wulan, J. Yan and Q. Jiang, *Adv. Mater.*, 2017, **29**, 1700001.

7 J. Han, X. Ji, X. Ren, G. Cui, L. Li, F. Xie, H. Wang, B. Li and X. Sun, *J. Mater. Chem. A*, 2018, **6**, 12974–12977.

8 D. Bao, Q. Zhang, F.-L. Meng, H.-X. Zhong, M.-M. Shi, Y. Zhang, J.-M. Yan, Q. Jiang and X.-B. Zhang, *Adv. Mater.*, 2017, **29**, 1604799.

9 J. Kong, A. Lim, C. Yoon, J. H. Jang, H. C. Ham, J. Han, S. Nam, D. Kim, Y.-E. Sung, J. Choi and H. S. Park, *ACS Sustainable Chem. Eng.*, 2017, **5**, 10986–10995.

10 X. Wu, L. Xia, Y. Wang, W. Lu, Q. Liu, X. Shi and X. Sun, *Small*, 2018, **14**, 1803111.

11 Z. Wang, F. Gong, L. Zhang, R. Wang, L. Ji, Q. Liu, Y. Luo, H. Guo, Y. Li, P. Gao, X. Shi, B. Li, B. Tang and X. Sun, *Adv. Sci.*, 2018, **5**, 1801182.

12 J. Han, Z. Liu, Y. Ma, G. Cui, F. Xie, F. Wang, Y. Wu, S. Gao, Y. Xu and X. Sun, *Nano Energy*, 2018, **52**, 264–270.

13 R. Zhang, H. Guo, L. Yang, Y. Wang, Z. Niu, H. Huang, H. Chen, L. Xia, T. Li, X. Shi, X. Sun, B. Li and Q. Liu, *ChemElectroChem.* 2019, **6**, 1014–1018.

14 H. Huang, L. Xia, R. Cao, Z. Niu, H. Chen, Q. Liu, T. Li, X. Shi, A. M. Asiri and X. Sun, *Chem. Eur. J.*, 2019, **25**, 1914–1917.

15 K. Jia, Y. Wang, Q. Pan, B. Zhong, Y. Luo, G. Cui, X. Guo and X. Sun, *Nanoscale Adv.*, 2019, **1**, 961–964.

16 Y. Wang, K. Jia, Q. Pan, Y. Xu, Q. Liu, G. Cui, X. Guo and X. Sun, *ACS Sustainable Chem. Eng.*, 2019, **7**, 117–122.

17 L. Zhang, L. Ding, G. Chen, X. Yang and H. Wang, *Angew. Chem.*, *Int. Ed.*, 2019, **58**, 2612–2616.

18 H. Huang, L. Xia, X. Shi, A. M. Asiri and X. Sun, *Chem. Commun.*, 2018, **54**, 11427–11430.

19 X. Zhu, Z. Liu, Q. Liu, Y. Luo, X. Shi, A. M. Asiri, Y. Wu and X. Sun, *Chem. Commun.*, 2018, **54**, 11332–11335.

20 X. Zhao, X. Lan, D. Yu, H. Fu, Z. Liu and T. Mu, *Chem. Commun.*, 2018, **54**, 13010–13013.

21 C. Lv, Y. Qian, C. Yan, Y. Ding, Y. Liu, G. Chen and G. Yu, *Angew. Chem.*, *Int. Ed.*, 2018, **57**, 10246–10250.

22 M. Shi, D. Bao, B. R. Wulan, Y. H. Li, Y. F. Zhang, J. M. Yan and Q. Jiang, *Adv. Mater.*, 2017, **29**, 1606550.

23 Z. Wang, Y. Li, H. Yu, Y. Yu, H. Xue, X. Li, H. Wang and L. Wang, *ChemSusChem*, 2018, **11**, 3480–3485.

24 J. Zhao, L. Zhang, X.-Y. Xie, X. Li, Y. Ma, Q. Liu, W.-h. Fang, X. Shi, G. Cui and X. Sun, *J. Mater. Chem. A*, 2018, **6**, 24031–24035.

25 W. Guo, Z. Liang, J. Zhao, B. Zhu, K. Cai, R. Zou and Q. Xu, *Small Methods*, 2018, 1800204.

26 L. Zhang, X. Ren, Y. Luo, X. Shi, A. M. Asiri, T. Li and X. Sun, *Chem. Commun.*, 2018, **54**, 12966–12969.

27 Y. Zhang, H. Du, Y. Ma, L. Ji, H. Guo, Z. Tian, H. Chen, H. Huang, G. Cui, A. M. Asiri, F. Qu, L. Chen and X. Sun, *Nano Res.*, 2019, **12**, 919–924.

28 X. Zhang, T. Wu, H. Wang, R. Zhao, H. Chen, T. Wang, P. Wei, Y. Luo, Y. Zhang and X. Sun, *ACS Catal.*, 2019, **9**, 4609–4615.

29 H. Huang, F. Gong, Y. Wang, H. Wang, X. Wu, W. Lu, R. Zhao, H. Chen, X. Shi, A. M. Asiri, T. Li, Q. Liu and X. Sun, *Nano Res.*, 2019, **12**, 1093–1098.

30 L. Xia, X. Wu, Y. Wang, Z. Niu, Q. Liu, T. Li, X. Shi, A. M. Asiri and X. Sun, *Small Methods*, 2019, **3**, 1800251.